

Microembossing of Ultra Fine-Grained Al

Xiao Guang Qiao¹, Nong Gao¹, Zakaria Moktadir², Michael Kraft² and Marco J. Starink¹

¹Materials Research Group, School of Engineering Sciences,

²School of Electronics and Computer Science,

University of Southampton, University Road, Highfield, Southampton, SO17 1BJ, UK.

Ultra fine grained (UFG) Al-1050 processed by equal channel angular pressing (ECAP) was embossed at both room temperature and 300 °C, with the aim of producing micro-channels. The cold embossing of Al foils is characterised by a partial pattern transfer, a large embossing force, channels with oblique sidewalls and a large failure rate of the mould. The hot embossing is characterised by straight channel sidewalls, fully transferred patterns and reduced loads which decrease the failure rate of the mould. Hot embossing of UFG Al shows a potential of fabrication of microelectromechanical system (MEMS) components with micro channels.

Keywords: Embossing; SPD; Al alloys; MEMS; microchannels.

1. Introduction

Microchannel patterned devices are extensively applied in microelectromechanical systems (MEMS) such as optical switches, microreactors, and micro heat exchangers. One way to fabricate such devices is to perform deep reactive ion etching (DRIE) on silicon wafers to get the components with micro scaled patterns [1]. The patterned silicon chips can be used as individual microparts or micro moulds allowing a polymer to be embossed [2]. However, silicon and polymers cannot meet the requirements of some applications. For instance, the materials inside micro heat exchangers are required to have a high thermal conductivity. The potential materials to replace silicon and polymers are metals, which generally have low thermal resistance, and preferentially low cost metals and alloys such as Cu and Al. These metals have been used extensively to fabricate traditional heat exchangers. Additionally, steel and titanium have been used [3,4,5,6] to fabricate micro heat exchangers with channel size in a scale of hundreds of micrometers by diamond machining.

Embossing of metals [7, 8, 9] including Al, stainless steel, Cu, brass and Zn78Al22 was attempted but many problems were observed such as uneven and rounded planks with ridges, a very high mould failure rate and a large embossing force required at room temperature. The problems reported in the literature are thought to be related, amongst others, to the difficulty in reliably embossing metals with conventional microstructures.

In severe plastic deformation (SPD), conventional microstructures materials are changed to submicron or nano-scaled ones [10, 11]. Equal channel angular pressing (ECAP) is one of the most effective processing method among the group of SPD methods [12,13]. It can be repeatedly performed on a single specimen because the specimen's cross section shape does not change during ECAP processing. The produced materials with submicron or nano-scaled grains are of low cost, low porosity, low oxide content and are safe compared to their

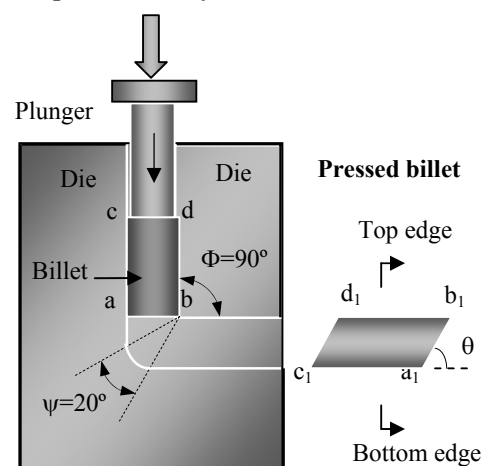


Fig. 1 Facility and principle of ECAP

counterparts obtained using gas condensation and mechanical alloying [10,13]. Although extensive research has been carried out on the microstructure and properties of ECAP processed alloys during the last decade [13,14, 15], the application of ECAP processed materials and the exploitation of the ultra fine grain structure are still of great interest to the research community.

Following on from our initial work on the processing of metallic foils with features at the scale of 5-50 μm [16] using ultra fine-grained (UFG) Al processed by ECAP, this study focuses on plastic flow of the UFG Al during embossing. The topography and the cross section of embossed channels are characterized by scanning electron microscopy (SEM) and focused ion beam (FIB).

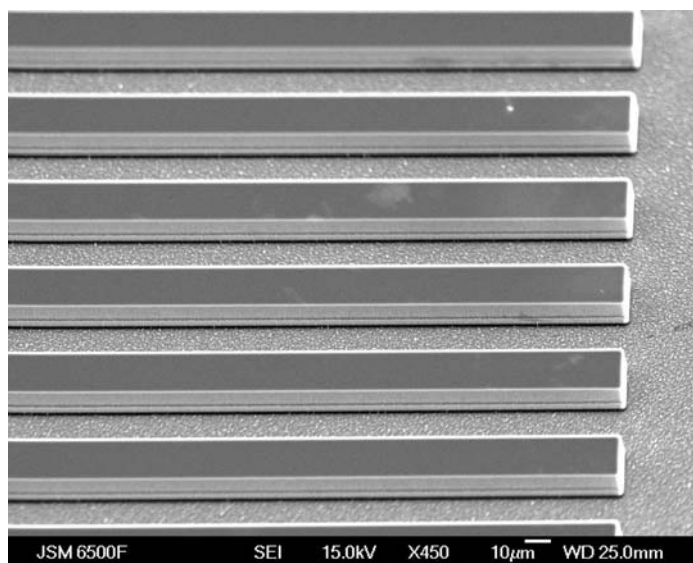


Fig. 2 SEM image of a micro silicon die with the channel depth of 10 μm and width of 25 μm .

2. Materials and Methods

2.1 Materials and processing

The present study was carried out on an Al-1050 alloy. Al-1050 is commercial purity aluminium with composition Al-0.18Fe-0.12Si (in wt. %) with further minor impurities. ECAP was performed at room temperature (Fig. 1) for up to 12 passes; further details on ECAP processing are provided in Ref [17].

The ECAP processed billet was machined along the longitudinal direction to 1mm thick disk shaped samples for embossing. The embossing process was carried out on the circular surface by the micro silicon die, i.e., a square plate of 14 mm side length and 0.5 mm thickness. The pattern on the centre of the micro silicon die is 10 mm long and 10 mm wide consisting of a series of parallel straight channels of 10 μm depth and 3-50 μm width with the same size grating. The micro silicon die was fabricated by deep reactive ion etching (DRIE), see Ref 16 for more details. The SEM image of the micro silicon die (Fig. 2) shows that the channel bottom is smooth. The measured depth of the channel is on average 10.03 μm .

The embossing process was carried out at ambient temperature and 300 $^{\circ}\text{C}$ on a 9510 Instron testing machine with maximum capacity of 10 kN (see Ref [16]). Platens and fixture were specially designed to fit the machine. A heating system and a cooling unit were specially designed to fit the machine. Embossing forces of 5 kN, 7 kN and 9 kN were used for cold embossing and a force of 3 kN was applied during embossing at 300 $^{\circ}\text{C}$ with a loading rate of 50 N/s, then held for 300 seconds. For hot embossing, the demoulding was performed at room temperature.

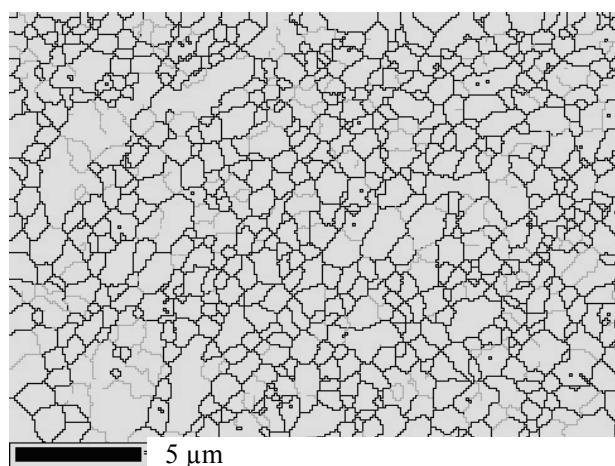


Fig. 3 EBSD analysis of Al-1050 alloys processed by twelve passes of ECAP

2.2 Characterization methods

Electron backscattered diffraction (EBSD) was used to characterize the microstructure as well as grain and subgrain boundary misorientation distribution in UFG Al-1050. The equipment used was a JEOL JSM6500F thermal field emission gun scanning electron microscope (FEG-SEM) equipped with an HKL EBSD detector and HKL Channel 5 software. The SEM accelerating voltage was set to 15 kV. The step size was 0.1 μm .

The FEG-SEM and an Olympus BH-2 optical microscope (OM) equipped with a Prosilica digital CCD camera were used to observe the cross-section and embossed surface of the UFG aluminium foils. A Carl Zeiss XB1540 focussed ion beam (FIB) was used to characterize the microstructure on the cross-section of the embossed foil. The FIB was operated at 30 kV with ion beam current of 200 pA.

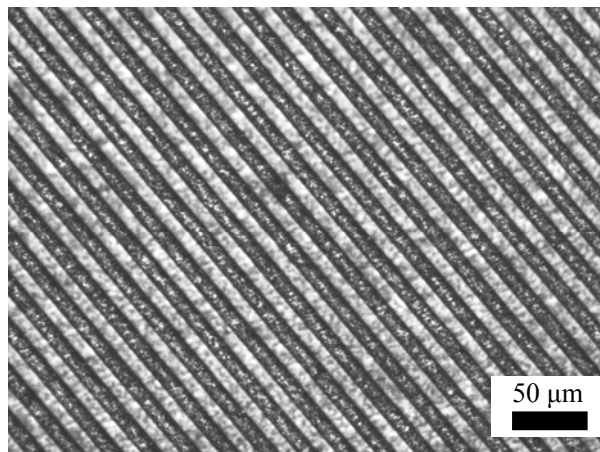


Fig. 4 Optical micrograph of the embossed topography of the UFG Al-1050 foil after two passes of ECAP.

3. Results

3.1 Microstructure of the UFG Al-1050

Fig. 3 shows the microstructure of Al-1050 alloy after 12 passes of ECAP as determined by EBSD. The grey fine (dark thick) lines represent low angle grain boundaries of which the misorientation angle is between 2° and 15° (greater than 15°). Misorientations angles less than 2° were ignored. The average grain size defined by the mean linear intercept length, was 0.88 μm after twelve passes of ECAP.

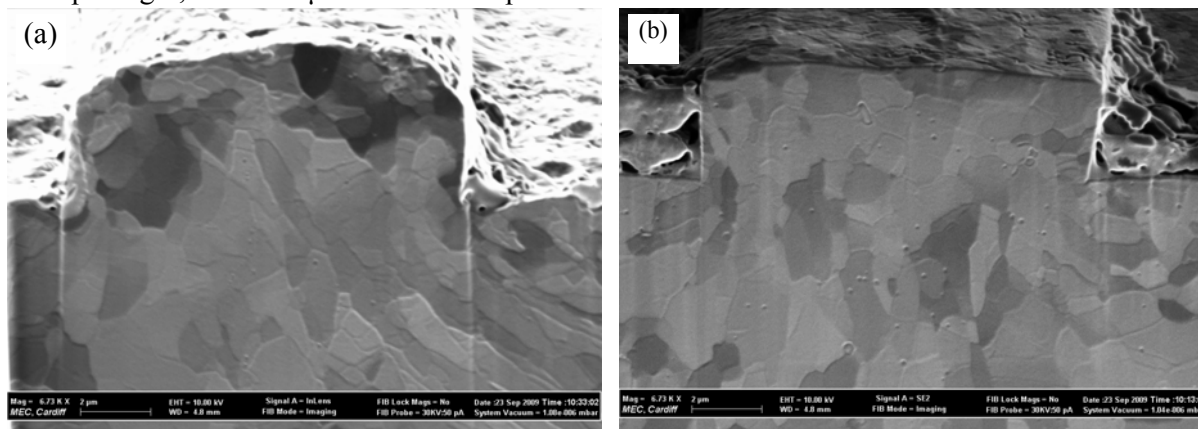


Fig. 5 FIB images of the cross section of the cold embossed Al-1050 foils processed by various passes of ECAP, a) two passes; b) eight passes.

3.2 Microstructure of cold embossed foils

For Al-1050 processed ECAP, the micro channels of the micro silicon die were partly transferred. For instance, one third of the foil surface was embossed when the embossing force was set at 5 kN. Fig. 4 shows the optical microscopy (OM) image of the embossed area of the foil. The channels on the micro silicon die were fully transferred to the foil surface.

Fig. 5 a) and b) show the cross section of cold embossed Al-1050 foils processed by two and eight passes of ECAP, respectively. In Fig. 5 a), the microstructure at the centre of the cross section

retains the typical microstructure of Al-1050 after two passes of ECAP, i.e. many shear bands are inclined at an angle of around 45° to the ECAP pressing direction; but near the top surface where strain is most intense, the shear bands are rotated and refined to equiaxed grains. In Fig. 5 b), the microstructure does not show any difference between the centre and the edges. They are all equiaxed grains, which are typical microstructure of Al-1050 after large number passes of ECAP.

The profile of microchannels of the eight passes of ECAP processed Al-1050 (Fig. 5 (b)) is sharper than that of the two passes of ECAP processed Al-1050 (Fig. 5 (a)). This is because the grain size of Al-1050 after eight passes of ECAP is smaller and grains are equiaxed [16]. However, the sidewalls of the microchannel in both embossed Al-1050 foils show an inclined angle to the channel bottoms, which causes demoulding to be difficult. Note that the bright contaminator at bottom left of the sidewall in Fig. 5 a) is irremovable resin.

3.3 Microstructure of hot embossed foils

Embossing at 300°C led to the whole surface of Al-1050 imprinted. Fig. 6 shows a typical SEM image of the surface of the UFG Al-1050 alloy foil embossed at 300°C . The flake-like contaminants are MoS_2 used as solid lubricants.

Cross sections of Al-1050 embossed at 300°C are shown in Fig. 7. Channels sidewalls of both alloys are straight, which is beneficial to demoulding. However, the channel edges of hot embossed Al-1050 are not perfectly sharp.

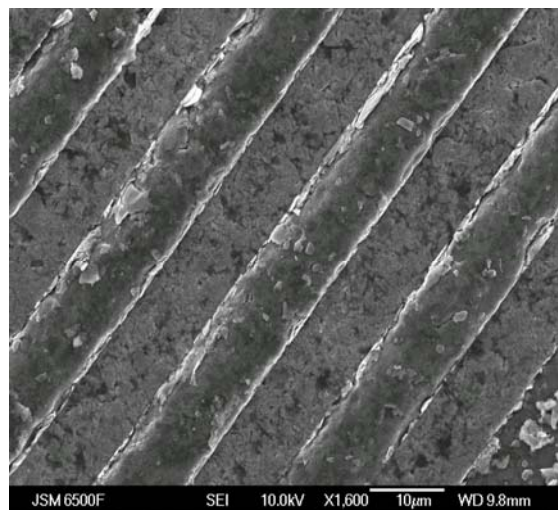


Fig. 6 SEM secondary electron images showing the topography of hot embossed UFG Al-1050 produced by four passes of ECAP. Channels are $10\mu\text{m}$ wide and $10\mu\text{m}$ deep.

4. Discussion

The objective of transferring the microchannels from the micro silicon die to the Al foils is to fabricate a micro heat exchanger. The next step after embossing is to bond the embossed Al foils through diffusion bonding. A sharp channel edge is essential to obtain a good bonding quality, as a rounded edge would reduce the contact area of two Al foils during diffusion bonding producing a weaker bonding with a notch like feature, which ultimately could lead to failure and leakage. A fine grain size is crucial to obtain sharp channel edges [16].

4.1 Cold embossing process

Al-1050 was partly embossed at room temperature. Only one third of the foil surface was patterned when the embossing force was set at 5 kN, rising to about 50% when the embossing force was set to 7kN or 9kN. Additionally, the failure rate due to the broken silicon mould dramatically increased when the embossing force was raised from 5 kN to 9 kN. The cross section of

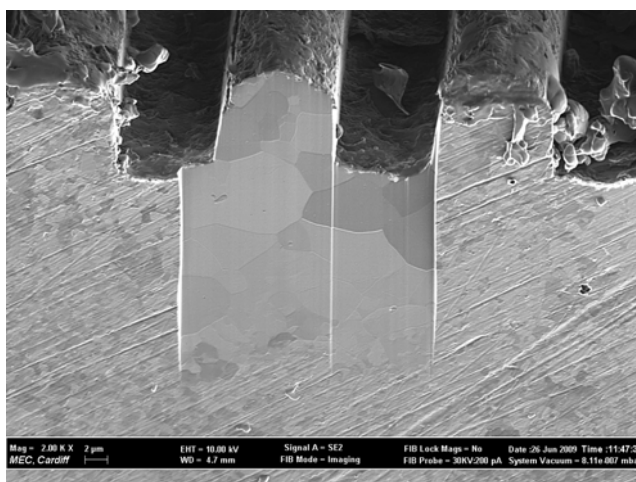


Fig. 7 FIB secondary electron image of cross section of hot embossed UFG Al-1050 produced by eight passes of ECAP.

cold embossed part of Al-1050 processed by eight passes of ECAP (see Fig. 5 (b)) shows a sharper edge and a flatter channel top than the Al-1050 processed by two passes of ECAP due to the smaller grain size. The cross section profile also appears to be of trapezoidal shape with a long side on the top.

4.2 Hot embossing process

During embossing at 300 °C, the pattern on the silicon die was fully transferred to Al-1050 by a reduced force of 3 kN. Small grains were thought to be crucial to obtain sharp channel edges and a flat channel top [16]. At high temperature, this deformation is dominated by grain rotation and grain boundary sliding, which differs from the mechanism of dislocation slip during deformation at room temperature. Moreover, the internal stress in the embossed channels generated during embossing would be recovered during holding time, which avoids forming a trapezoidal channel after demoulding.

The above analysis suggests that hot embossing leads to straight sidewalls of channels and easy demoulding. However, releasing the mould from the hot embossed Al foils were more difficult than from cold embossed ones. This is because demoulding was carried out at room temperature and Al foils had a much more shrinkage than the micro silicon mould. As shown in **Error! Reference source not found.**, the micro silicon mould and the Al foil are supposed to be 10 mm wide at 300 °C. They would shrink to 9.9916 mm and 9.9296 mm since the coefficient of linear thermal expansion for Si and Al at 20 °C are $2.6 \times 10^{-6}/^{\circ}\text{C}$ and $23 \times 10^{-6}/^{\circ}\text{C}$ [18], respectively. The Al foil would have 62 μm more shrinkage than the micro silicon mould so that the embossed Al foil was restricted by a tensile stress and difficult to be released from the micro silicon mould. The stress release occurring when the Al foils detach the micro silicon mould increases the possibility of scratching the channel top. Demoulding at the embossing temperature may avoid this shrinkage problem and will lead to a smooth mould release process. In the present study, the mould release was performed manually at room temperature as automatic tools for hot mould release were not available.

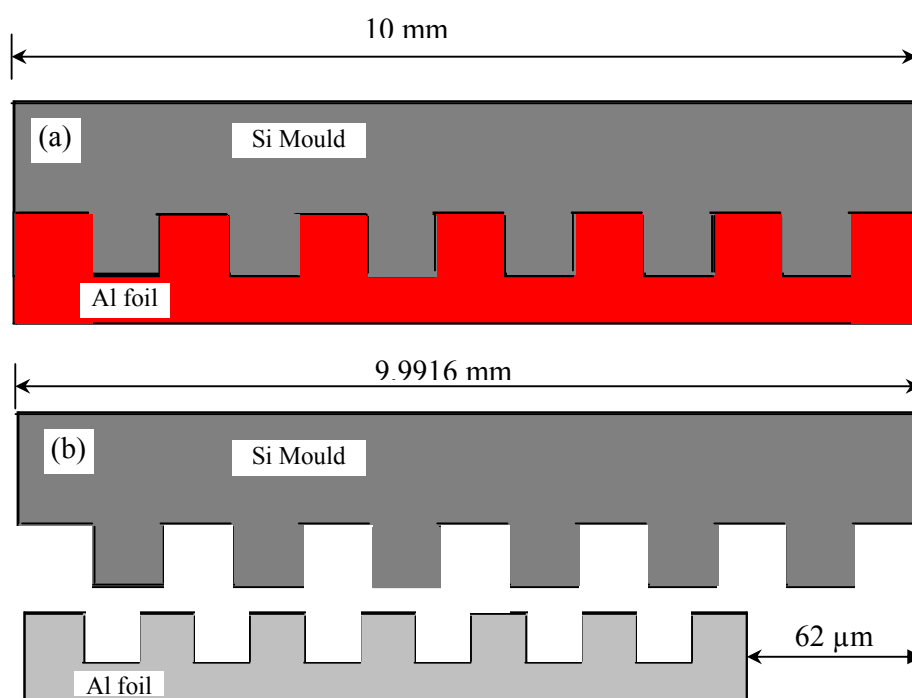


Fig. 8 Schematically illustration of thermal expansion of an Al foil and a Si mould during hot embossing and demoulding. (a) Embossing at 300 °C, (b) Demoulding at room temperature.

5. Conclusions

A novel process for the fabrication of a microelectromechanical systems (MEMS) metallic component with features smaller than 10 μm and high thermal conductivity was investigated. In the first stage of processing, an ultra fine-grained (UFG) Al-1050 was produced by equal channel angular pressing (ECAP). Conclusions are drawn as follows:

- 1) Cold embossing of the UFG Al-1050 processed by ECAP leads to a high failure rate of micro silicon mould and an incomplete pattern transaction from the silicon mould to the foil.

- 2) The partly embossed Al-1050 at room temperature shows channels with an unflat sidewall, which causes difficulty of demoulding.
- 3) Embossing of UFG Al-1050 at 300 °C produces smooth channels with straight sidewalls. The pattern on the micro silicon mould is fully transferred to the foil surface.
- 4) Hot embossing of UFG Al shows a good potential for application in microdevice fabrication if a proper loading rate and a superplastic temperature are identified and an automatic hot demoulding tool is available.

Acknowledgements

This work was part-funded by the Engineering and Physical Sciences Research Council under Grant No. EP/D00313X/1. The FIB work was funded under Grant No. EP/F056745/1. Author XGQ thanks ORSAS and School of Engineering Sciences of University of Southampton for additional studentship funding. Prof. S.M. Spearing and Dr. Liudi Jiang (University of Southampton) are gratefully acknowledged for valuable discussion. Dr. Georgi Lalev (University of Cardiff) is gratefully acknowledged for FIB work.

Reference:

-
- [1] C. Chang, Y. F. Wang, Y. Kanamori, J. J. Shih, Y. Kawai, C. K. Lee, K. C. Wu and M. Esashi: *J. Micromech. Microeng.* 15 (2005) 580–85.
 - [2] D. Hardt, B. Ganesan, M. Dirckx, G. Shoji, K. Thaker and W. Qi: *Innovation in Manufacturing Systems and Technology IMST* (2005) 01
 - [3] C.R. Friedrich and S.D. Kang: *Preci. Eng.* 16 (1994) 56-59.
 - [4] K. Schubert, J. Brandner, M. Fichtner, G. Linder, U. Schygulla and A. Wenka: *Microscale Thermophys. Eng.* 5 (2001) 17–39.
 - [5] J. J. Brandner, E. Anurjew, L. Bohn, E. Hansjosten, T. Henning, U. Schygulla, A. Wenka and K. Schubert: *Exp. Therm Fluid Sci.* 30 (2006)801-09.
 - [6] W. Bier, W. Keller, G. Linder, D. Seidel and K. Schubert: *Winter Annual Meeting of the American Society of Mechanical Engineers* (Dallas, TX, USA 25-30 November 1990) pp189-97.
 - [7] T. Otto, A. Schubert, J. Böhm and T. Gessner: *Proc. SPIE – Int. Society for Optical Engineering vol 4179* ed. S.H. Lee and E.G. Johnson (Bellingham, WA: Society of Photo-Optical Instrumentation Engineers) pp 96–106.
 - [8] J. Jiang, F. Mei, W.J. Meng, G.B. Sinclair and S. Park: *Microsyst. Technol.* 14 (2008) 815–819.
 - [9] J. Böhm, A. Schubert, T. Otto and T. Burkhardt: *Microsystem Tech.* 7 (2001) 191-195.
 - [10] R.Z. Valiev, Y. Estrin, Z. Horita, T.G. Langdon, M.J. Zehetbauer and Y.T. Zhu: *JOM* 58 (2006) 33-39.
 - [11] M.J. Starink, X.G. Qiao, J. Zhang and N. Gao: *Acta Mater.* 57 (2009) 5796-5811.
 - [12] R. Z. Valiev, R. K. Islamgaliev and I. V. Alexandrov: *Prog. Mater. Sci.* 45 (2000)103-189.
 - [13] R. Z. Valiev and T.G. Langdon: *Prog.Mater. Sci.* 51 (2006) 881–981.
 - [14] N. Gao, M. J. Starink, M. Furukawa, Z. Horita, C. Xu and T.G. Langdon : *Mater. Sci. Eng. A* 410-411 (2005)303-07.
 - [15] B. Baretzky et al: *Rev. Adv. Mater. Sci.* 9 (2005) 45-108.
 - [16] X.G. Qiao, N. Gao, Z. Moktadir, M. Kraft and M. J. Starink: *J. Micromech. Microeng.* 20 (2010) 045029.
 - [17] X. G. Qiao, M. J. Starink and N. Gao: *Mater. Sci. Eng. A* 513–514 (2009) 52–58.
 - [18] G.W.C. Kaye and T. H. Laby: *Tables of physical and chemical constants*, (Longman, Harlow, UK, 16th edition, 1995).